

# Energy generation from domestic wastewater using sandwich dual-chamber microbial fuel cell with mesh current collector cathode

J. A. Adeniran<sup>1</sup> · R. Huberts<sup>2</sup> · J. J. De-Koker<sup>3</sup> · O. A. Arotiba<sup>4</sup> · O. F. Olorundare<sup>4</sup> · E. Van-Zyl<sup>5</sup> · S. C. Du-Plessis<sup>6</sup>

Received: 23 February 2016/Revised: 22 April 2016/Accepted: 27 June 2016/Published online: 7 July 2016  
© Islamic Azad University (IAU) 2016

**Abstract** A sandwich domestic wastewater-fed dual-chamber microbial fuel cell (MFC) was designed for energy generation and wastewater treatment. The generated power density by the MFC was observed to increase with increasing chemical oxygen demand (COD) of the domestic wastewater. The maximum power density was  $251 \text{ mW m}^{-2}$  when the COD was  $3400 \text{ mg L}^{-1}$  at a current density of  $0.054 \text{ mA cm}^{-2}$  and external resistance of  $200 \Omega$ . These values dropped to  $60 \text{ mW m}^{-2}$  (76 % lower) and  $0.003 \text{ mA cm}^{-2}$  using wastewater 91 % diluted to  $300 \text{ mg L}^{-1}$  COD. Maximum removals were: COD, 89 %; nitrite, 60 %; nitrate, 77 %; total nitrogen, 36 %; and phosphate, 26 %. Coulombic efficiency ranged from 5 to 7 %. The use of full-strength domestic wastewater reduces

cost, and with improved reactor design, the ultimate goal of large-scale operation could be achieved.

**Keywords** Domestic wastewater · Mesh current collector cathode · Microbial fuel cells · Power generation

## Introduction

In the early days of microbial fuel cell (MFC) research, most of the studies were carried out using the conventional dual-chamber MFC. However, the recent trend in MFC research involves the use of single-chamber MFCs. This is in accordance with reports of higher power and current densities generated from single-chamber MFCs compared with dual-chamber MFCs. Higher internal resistance and electron acceptor limitations are among the major factors that restrict power generation in dual-chamber MFCs. In MFC studies, in a bid to increase power generation, the impact of various materials used in the construction of reactors has been investigated. The use of catalyzed cathodes built around mesh current collectors used in single-chamber MFCs has been reported to increase power generation significantly (Luo et al. 2011; Zhang et al. 2009, 2010, 2011). Mesh pore sizes also play an important role in increasing power density in MFCs. In a study by Zhang and co-workers (2011), the effect of cathode mesh pore size on power generation was ascertained, using five stainless steel meshes of different pore sizes (30, 50, 70, 90 and 120), treated with poly(dimethyl siloxane) (PDMS) and Pt, as cathode in a single-chamber cubic-shaped MFC. The results indicated direct proportionality between pore sizes and power density. Mesh 30 recorded the highest maximum power density of  $1616 \pm 25 \text{ mW m}^{-2}$ , while the lowest power density of  $599 \pm 57 \text{ mW m}^{-2}$  was

✉ J. A. Adeniran  
nikjocrown2000@yahoo.com

<sup>1</sup> Department of Civil Engineering Technology, University of Johannesburg, P.O. Box 17011, Doornfontein, Johannesburg 2028, South Africa

<sup>2</sup> Department of Chemical Engineering Technology, University of Johannesburg, P.O. Box 17011, Doornfontein, Johannesburg 2028, South Africa

<sup>3</sup> Sustainable Energy Technology and Research Centre, SeTAR, University of Johannesburg, P.O. Box 17011, Doornfontein, Johannesburg 2028, South Africa

<sup>4</sup> Department of Applied Chemistry, University of Johannesburg, P.O. Box 17011, Doornfontein, Johannesburg 2028, South Africa

<sup>5</sup> Department of Biotechnology and Food Technology, University of Johannesburg, P.O. Box 17011, Doornfontein, Johannesburg 2028, South Africa

<sup>6</sup> Metallurgy Department, University of Johannesburg, P.O. Box 17011, Doornfontein, Johannesburg 2028, South Africa

obtained with mesh 120 which has the smallest pore size. A further investigation into the use of these mesh pore sizes may be helpful in increasing the power generation and efficiency of MFCs.

Despite the aforementioned advantages of single-chamber MFCs over dual-chamber MFCs, the shortcomings of lower coulombic efficiency (in comparison with dual chambers) (Zhang et al. 2009; Liu and Logan 2004) and leakage of the anode solution through the cathode (Zhang et al. 2009) reported in single-chamber MFCs need to be overcome to maximize the potential of MFC technology for energy generation and wastewater treatment. An improvement in the design of dual-chamber MFCs in terms of architecture and materials of construction may be a viable alternative way of overcoming the limitations of single-chamber MFCs. In this study, a dual-chamber MFC with reduced electrode spacing was developed and tested for energy generation from domestic wastewater. In addition, the impact of wastewater organic materials concentration (wastewater concentration) in the anode chamber on energy generation was ascertained.

Mesh current collectors have been used previously as cathode in single-chamber MFC studies (Xia et al. 2013; Luo et al. 2011; Zhang et al. 2009, 2010, 2011). However, to the best of the knowledge of authors, this is the first study involving a combined use of mesh current collector cathode and sandwich electrodes architectures in a dual-chamber MFC. This research was conducted from 2013 to 2014, in the Bio-process Research laboratory of the Faculty of Engineering and the Built Environment, University of Johannesburg, South Africa.

## Materials and methods

### Cathode

The cathode was constructed from stainless steel mesh 20 type 304 (0.37 mm diameter, 0.90 mm opening, 737 MPa tensile strength and 39 % elongation). The stainless steel mesh was supplied by Ludowisi Meshcape, South Africa (SA). The cathode was uncatalyzed, with a projected surface area of 36 cm<sup>2</sup>, a thickness of 0.72 mm and a total weight of 6.60 g. Details of the mesh material used are provided in Table 1.

### MFC construction and operation

#### *Sandwich electrode membrane electrode configuration, SEMEC*

A sandwich consisting of the anode (non-wet proof carbon fabric, 1071HCB, Avcarb, NJ), the proton exchange

membrane (PEM) (CMI 7000S, Membranes International Inc., NJ) and the cathode was glued to the anode chamber (polyethylene wide-mouth bottle). This is illustrated schematically in Fig. 1. The anode compartment had a total volume of 2000 mL and was filled with 1500 mL of domestic wastewater (1500 mL empty bed volume). The anode had a surface area of 36 cm<sup>2</sup>, and the sandwich weighed 10.6 g. Thus, the PEM employed was treated with 5 % NaCl solution for 12 h to allow for membrane surface activation and expansion. Thereafter, the entire structure was placed in a temperature-regulated water bath (Eco-bath, Labotech, South Africa) containing the cathode solution. The water bath's in-built circulator replenished the dissolved oxygen used as the electron acceptor at the cathode.

### MFC operation

The reactor was inoculated with primary sludge and domestic wastewater from Daspoort wastewater treatment works, Pretoria, South Africa, and subsequently fed with domestic wastewater after a repeatable current production had been established. The reactor was a semi-continuous one operated on a long fed batch cycle (fed with 500 mL fresh influent once a week), at 35 °C. Hence, a wastewater residence time of 3 weeks was achieved. The cathode solution was maintained at pH of approximately 1.88, while the anode solution was operated at an average pH of 7.5. The CODs of the influent and effluent were determined using Hach COD system (Hach Co., Loveland, CO, USA).

### MFC calculations and measurements

The voltage (V) across the external resistor was measured at 5-min intervals after a pseudo-steady state had been established. The power ( $P = IE_{MFC}$ ) and current ( $I = \frac{E_{MFC}}{R_{ext}}$ ) produced by the reactor were determined by measuring the potential across the external resistor, as described by Logan et al. (2006).  $E_{MFC}$  and  $R_{ext}$  represent the cell potential (volts) and external resistance or load (ohm), respectively. Polarization and power density curves were obtained by varying the external circuit resistance from 2400 to 50 Ω in decreasing order. Power and current densities were normalized to the projected surface area of the cathode (36 cm<sup>2</sup>) at  $R_{ext}$  200 Ω, except when stated otherwise.

The MFC internal resistance was calculated using the polarization slope method. This was achieved by calculating the slope of the polarization curve, using the formula:

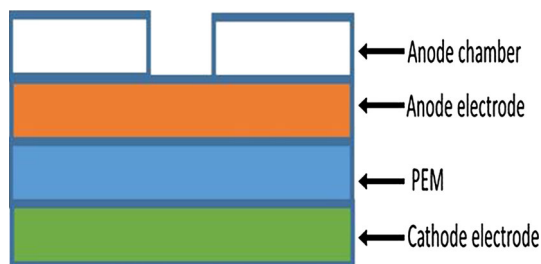
$$R_{int} = \frac{\Delta E}{\Delta I} \quad (1)$$



**Table 1** Mesh material and chemical composition

Material type	Component element <sup>a</sup>	Specification (AISI 304) wt% <sup>a</sup>		Average specification <sup>a</sup> wt%
		Max	Min	
AISI 304 stainless steel. #20	C	0.08	–	0.051
	Mn	2.0	–	1.23
	Si	–	0.1	0.69
	P	0.045	–	0.021
	Ni	10.5	8.0	9.78
	Cr	20	18	18.91
	S	0.03	–	0.018

<sup>a</sup> Mesh information supplied by the manufacturer

**Fig. 1** Schematic representation of MFC design

where  $\Delta E$  is the change in voltage and  $\Delta I$  is the change in current. The coulombic efficiency (CE) was determined from the COD removed per cycle of operation (Logan et al. 2006) using the following formula:

$$CE = \frac{M_S I t_b}{F b_{es} V_{an} \Delta_{COD}} \quad (2)$$

where  $M_S$  is the molecular weight of substrate ( $\text{g mol}^{-1}$ ),  $I$  is the current density ( $\text{mA cm}^{-2}$ ),  $t_b$  is the operation time (h),  $F b_{es}$  is the Faraday's constant [ $(96,500 \text{ }^\circ\text{C/mol}^-)$  ( $8 \text{ mol}^-/\text{mol}$ )],  $V_{an}$  is the volume of the anode (L) and  $\Delta_{COD}$  is the change in COD ( $\text{g L}^{-1}$ ).

### Characterization of electrodes

The characterization of the electrodes was carried out using electrochemical characterization (cathode) and scanning electron microscope (SEM) for the anode.

### Electrochemical characterization

Electrochemical characterization [open circuit potential (OCP) and cyclic voltammetry (CV)] of the mesh electrode was conducted on an Ivium CompactStat potentiostat

(Netherlands). A three-electrode system consisting of a stainless steel mesh (cathode in the MFC) as working electrode, a platinum counter electrode and an Ag/AgCl reference electrode (RE-5B; BASi; West Lafayette, IN) was employed. The tests were conducted using three different solutions. The first solution was a mixture of 50 % cathode solution (water and sulfuric acid) and 50 % 10 mM phosphate buffer solution (PBS) (made up of  $\text{Na}_2\text{HPO}_4$   $0.458 \text{ g L}^{-1}$  +  $\text{Na}_2\text{HPO}_4 \cdot \text{H}_2\text{O}$   $0.245 \text{ g L}^{-1}$ ). The second solution consisted of 50 % 50 mM PBS and 50 % cathode solution, while the third solution was the cathode solution without a supporting electrolyte. The cyclic voltammetry scan rate was  $+0.50 \text{ mV s}^{-1}$  and the potential was scanned from  $+1.0$  to  $-0.4 \text{ V}$ .

### Electron microscopy examination

Scanning electron microscope images of the anode were taken to observe biofilm growth using a VEGA3 TESCAN (Tescan Brno-Kohoutovice, Czech Republic). The anode (working and control) were cut into small pieces (about  $1 \text{ cm} \times 1 \text{ cm}$ ) and fixed overnight in 2.5 % paraformaldehyde and 1.5 % glutaraldehyde in 0.1 M cacodylate buffer, pH 7.4 at  $4 \text{ }^\circ\text{C}$ . They were washed three times in the buffer, dehydrated in graded ethanol solutions, and dried at the critical point using carbon dioxide (Liu and Logan 2004). Thereafter, the samples were gold sputter-coated using an Emscope SC 500 gold coater.

### Nutrient removal analysis

In order to determine the efficiency of the reactor for wastewater treatment, concentrations of nitrate, nitrite, total nitrogen, and phosphate were analyzed in the influents and effluents using Hach techniques (Hach Co., Loveland, CO, USA.). Prior to the analysis, the samples were centrifuged to ensure homogeneity. All analyses were carried out in triplicate and the average reported to ensure reproducibility of the results. For nitrate (cadmium reduction method,  $0.3\text{--}30.0 \text{ mg L}^{-1} \text{ NO}_3^- \text{N}$ ); nitrite (ferrous sulfate method, NitriVer2,  $2\text{--}250 \text{ mg L}^{-1} \text{ NO}_2^-$  reagent powder pillows); total nitrogen (persulfate digestion method,  $2\text{--}150 \text{ mg L}^{-1} \text{ N}$ , test tube and vials); and phosphate (molybdovanadate method  $0.3\text{--}45.0 \text{ mg L}^{-1} \text{ PO}_4^{3-}$ , reagent solution), the methods indicated in the respective brackets were used for the analyses.

The nutrient removals were determined using the formula in Eq. (3):

$$C_{\text{removed}} = \frac{C_{\text{influent}} - C_{\text{effluent}}}{C_{\text{influent}}} \times 100 \% \quad (3)$$



where  $C_{\text{removed}}$  is the nutrient removed (%),  $C_{\text{influent}}$  is the influent nutrient concentration ( $\text{mg L}^{-1}$ ) and  $C_{\text{effluent}}$  is the effluent nutrient concentration ( $\text{mg L}^{-1}$ ).

### Wastewater organic matter concentration measurement

The influent and effluent organic matter concentrations were determined by carrying out COD analysis; hence, wastewater COD concentration was used as a measure of organic matter concentration in this study. The analyses were done in triplicate and the average reported, using the Hach COD system (Hach Co, Loveland, CO, USA). The wastewater strength was varied from 3400 to 300  $\text{mg L}^{-1}$  by dilution with deionized water to ascertain the effect of substrate organic matter concentration on power generation. The COD removal (%) was calculated using the formula in Eq. (4):

$$X_r = \frac{X_i - X_e}{X_i} \times 100\% \quad (4)$$

where  $X_r$  is the COD removed (%),  $X_i$  is the influent COD ( $\text{mg L}^{-1}$ ) and  $X_e$  is the effluent COD ( $\text{mg L}^{-1}$ ).

## Results and discussion

### Organic matter concentration and power generation

The effect of wastewater COD concentration on power production was examined by comparing the power density at the highest substrate COD concentration (PDH) and the polarization (PCH) curves with those at the lowest COD concentration (PDL and PCL) (Fig. 2a). The maximum power generation from the MFC at various COD concentrations is represented in Fig. 2b.

Maximum power density of  $251 \text{ mW m}^{-2}$  and current density of  $0.059 \text{ mA cm}^{-2}$  were generated at the highest COD ( $3400 \text{ mg L}^{-1}$ ). In turn, the lowest power density ( $60 \text{ mW m}^{-2}$ ) and current density ( $0.03 \text{ mA cm}^{-2}$ ) were generated when wastewater of the lowest COD concentration of  $300 \text{ mg L}^{-1}$  was fed (Fig. 2a), representing a 76 % drop in power density. Throughout the course of the experiments, a general trend of reduction in power production with COD reduction was observed (Fig. 2b). This is similar to findings in previous studies (Zhong et al. 2011; Rodrigo et al. 2007) where high substrate concentration increased power density in MFCs. This finding is also consistent with findings in some previous studies that power generation in MFCs depends on wastewater concentration (Liu et al. 2005; Min et al. 2005). In the same vein, the observation is similar to reports of increased power generation with feed concentration (Moon et al. 2006), where highest power and current densities of  $0.36 \text{ W m}^{-2}$  and  $1.6 \text{ A m}^{-2}$ , respectively, were reported at the highest fuel concentration of  $300 \text{ mg L}^{-1}$ . The results, however, differ from the findings by Zhong et al. (2011) where COD concentration was found not to be the only limiting factor in power generation. In their study, Zhong and co-workers investigated power generation at three organic loading rates (OLRs), viz.  $6.00$ ,  $3.20$  and  $1.55 \text{ kg COD m}^{-3} \text{ day}^{-1}$ . The lowest power density of  $74.0 \pm 1.8 \text{ mW m}^{-2}$  ( $0.65 \pm 0.02 \text{ mW}^{-3}$ ) was recorded at  $6.00 \text{ kg COD m}^{-3} \text{ day}^{-1}$ , followed by  $92.1 \pm 3.3 \text{ mW m}^{-2}$  ( $0.081 \pm 0.03 \text{ mW}^{-3}$ ) at  $1.55 \text{ kg COD m}^{-3} \text{ day}^{-1}$ , and with a maximum power density of  $115.5 \pm 2.7 \text{ mW m}^{-2}$  ( $1.0 \pm 0.02 \text{ mW}^{-3}$ ) being generated at  $3.20 \text{ kg COD m}^{-3} \text{ day}^{-1}$ . It was reported that factors such as poisoning of the catalyst (Pt) at high organic matter concentration and fouling of the catalyst layer by biofilm could be partly responsible for the development. However, in this study no catalyst was applied to the electrodes, which could be responsible for the different

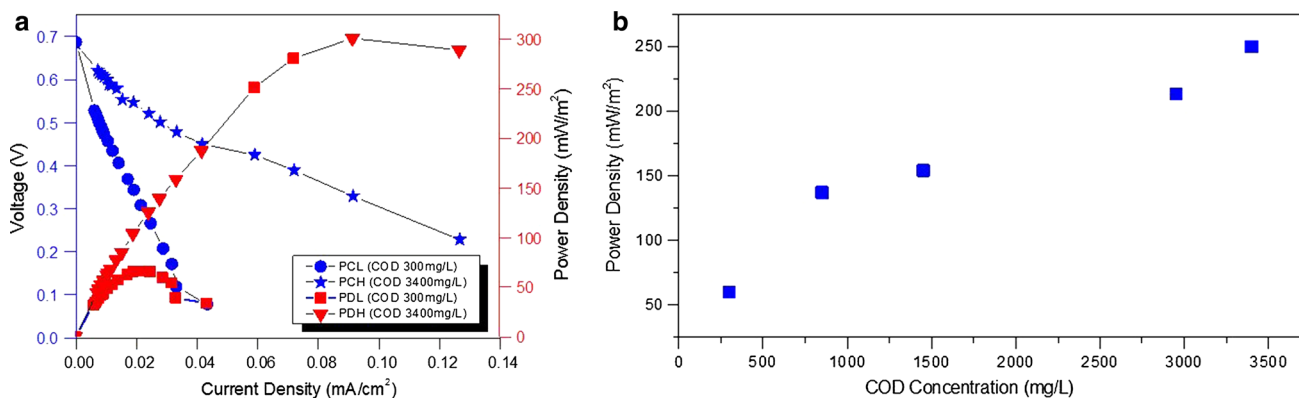


**Fig. 2** a Polarization and power curves at lowest and at highest COD. b Power density as a function of COD concentration

**Table 2** Selected maximum power densities using natural wastewater in MFCs

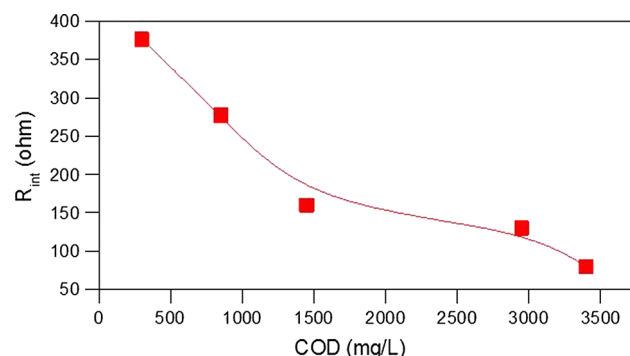
Substrate	MFC type	Maximum power density ( $\text{mW m}^{-2}$ )	References
Brewery wastewater	Air cathode single chamber	528	Feng et al. (2008)
Corn stover biomass	Air cathode single-chamber bottle	406	Wang et al. (2009)
Beer brewery wastewater	Air cathode single chamber	264	Wen et al. (2009)
Swine wastewater	Air cathode single chamber	261	Min et al. (2005)
Domestic wastewater	Air cathode single chamber without PEM	146	Liu and Logan, (2004)
Molasses wastewater	Anaerobic baffled stacking	115.5	Zhong et al. (2011)
Swine wastewater	Dual chamber	45	Min et al. (2005)
Urban wastewater	Dual chamber with salt bridge	25	Rodrigo et al. (2007)
Full-strength domestic wastewater	Sandwich dual chamber	251	This work

observations. The maximum average power density of  $251 \text{ mW m}^{-2}$  obtained in this study is higher than the power densities reported in previous natural wastewater-fed dual-chamber MFC studies:  $63 \text{ mW m}^{-2}$  (Min and Logan 2004) using domestic wastewater in a flat plate MFC;  $45 \text{ mW m}^{-2}$  (Min et al. 2005) when swine wastewater was used as substrate; and  $25 \text{ mW m}^{-2}$  (Rodrigo et al. 2007) using urban wastewater.

It can be seen from Table 2 that the maximum power density reported in this work compares favorably with that of most studies in which natural wastewaters were used as substrates in MFCs. This suggests that the sandwich dual-chamber MFC designed for this work is efficient in terms of power generation, taking into consideration the fact that dual-chamber MFCs are known to generate lower power densities than single-chamber MFCs (Logan 2008).

### Internal resistance

The internal resistance ( $R_{\text{int}}$ ) of the reactor was determined using the polarization slope method (Logan 2008). The internal resistances recorded were inversely proportional to the COD concentration (Fig. 3), with the highest  $R_{\text{int}}$  of  $376 \Omega$  recorded at  $300 \text{ mg L}^{-1}$  COD concentration and the

**Fig. 3** Internal resistance relationship with substrate concentration

minimum  $R_{\text{int}}$  of  $80 \Omega$  at a COD concentration of  $3400 \text{ mg L}^{-1}$ . This is consistent with the results of Feng et al. (2008) who found that  $R_{\text{int}}$  decreased with an increase in COD concentration. The minimum  $R_{\text{int}}$  of  $80 \Omega$  is high compared with some of the previously reported results (Fan et al. 2007; Cheng et al. 2006), but lower than the  $1632 \Omega$  reported by You et al. (2006) when permanganate was used as the electron acceptor in a dual-chamber MFC. A maximum  $R_{\text{int}}$  of  $376 \Omega$  was recorded in this study (Fig. 3). This is higher than  $159 \pm 11$ ,  $184 \pm 15$  and  $216 \pm 8 \Omega$  (using lactic acid, acetic acid and ethanol, respectively, as substrates) and equal to  $376 \pm 30 \Omega$  (succinic acid substrate) reported in the study by Kiely and fellow workers (2011). However, it is significantly lower than  $2769 \pm 318 \Omega$  obtained in the same study (Kiely et al. 2011) when formic acid was used as a substrate. Bearing in mind that solution conductivity affects power generation in MFCs due to its impact on ionic flow (Logan 2012) and the fact that domestic wastewater is known for low conductivity, full-strength domestic wastewater ( $698 \pm 81 \mu\text{s cm}^{-1}$ ) was used as substrate in this study. The low substrate conductivity is believed to be responsible for the relatively high internal resistance ( $R_{\text{int}}$ ).

From the polarization curve in Fig. 4, it can be deduced that activation losses were prominent from 0 to  $0.033 \text{ mA cm}^{-2}$ , as depicted by the first high gradient (I) in region A. The ohmic region between  $0.033$  and  $0.072 \text{ mA cm}^{-2}$ , denoted by region B, can be observed to be characterized by the relatively steady rise in gradient, and the mass transport losses can be observed from  $0.072$  to  $0.127 \text{ mA cm}^{-2}$ , characterized by a steep rise in gradient (region C). The magnitude of the activation loss observed in this figure could be attributed to the use of an uncatalyzed electrode and the relatively high energy required for the oxidation and reduction reaction due to the high COD concentration of the wastewater (Logan 2008). Ohmic losses represent one of the major challenges to be overcome in the design of a scalable MFC (Logan 2008).



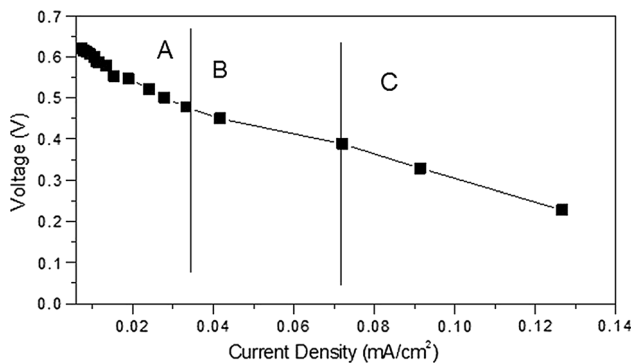


**Fig. 4** Polarization curve of the MFC at the highest COD ( $3400 \text{ mg L}^{-1}$ )

Although a sandwich MFC design known for reduced internal resistance (Liu and Logan 2004) was used for the experiments, the use of a membrane (PEM) in this study could be responsible for the relatively large interval of ohmic losses observed in the polarization curve in Fig. 4 (Logan et al. 2006). The observation of mass transport losses in the polarization curve is an indication of the need to improve the reactant and product flux on the electrodes (Logan 2008).

#### Nutrient removal and coulombic efficiency

Table 3 presents the wastewater treatment efficiency using the percentage of nutrients removed as an indicator. The removal of nitrate and phosphate is attributed to a process caused by the bacteria consortium in the wastewater. The nitrate removal is also an indication of a denitrification process in the reactor.

The reason for the relatively lower total nitrogen removal (36 %), compared with nitrate (77 %) and nitrite (66 %), is not well understood at this stage. However, since total nitrogen contains both organically bound nitrogen and oxidizable nitrogen (nitrite and nitrate) it is

**Table 3** Summary of the wastewater treatment efficiency analysis of the MFC

Parameter ( $\text{mg L}^{-1}$ )	Percentage removed
COD	89
$\text{NO}_3^-$	77
$\text{NO}_2^-$	60
N	36
$\text{PO}_4^{3-}$	26

assumed that endogenous decay of the microorganisms in the wastewater might have resulted in the release of organically bound nitrogen, as noted by Bahadoorsingh (2010). This happens during a long retention time and with a low ratio of substrate to microorganisms, leading to autolysis which causes a release of large quantities of organic matter (Miura et al. 2007). It is hypothesized that the relatively long residence time of the wastewater in the MFC (3 weeks) could favor endogenous decay. This phenomenon will lead to the release of the organically bound nitrogen component of the total nitrogen, hence its relatively higher concentration in the effluent compared with nitrite and nitrate.

A better measure of the extent of wastewater treatment in the MFC is COD measurement. A maximum COD removal of 89 % was recorded in this study, signifying an efficient wastewater treatment. The high COD removal (89 %) and low CE values (5–7 %) also support the assumption of nutrient removal by bacteria, possibly other than the exoelectrogenic bacteria. A similar finding was made by He et al. (2005), who recorded a soluble chemical oxygen demand (SCOD) removal of 90 % and CEs of 0.7–8.1 % in an up flow MFC. The findings were attributed to oxidation of the anodic substrates by bacteria other than the exoelectrogens.

From Fig. 5, it can be seen that the CE during the course of the experiment ranged from 5 to 7 %. The maximum CE was recorded between wastewater concentrations of 300 and  $800 \text{ mg L}^{-1}$ , with the lowest CE recorded between 2200 and  $3400 \text{ mg L}^{-1}$ . The relationship between CE and substrate concentration is inverse, which is similar to the observations by Min and coworkers (2005). The CE obtained in this study is poor (maximum of 7 %), and this suggests that the reactor was not efficient in converting the organic matter in wastewater to energy. It is also an indication that the design needs to be further optimized for improved energy generation. The relatively longer cycle of operation (7 days) could be partly responsible for the low CE recorded because of the potential increase in oxygen influx to the anode due to the increase in operation time. This is consistent with the findings of Feng et al. (2008). Further efforts need to be made to prevent the influx of oxygen into the anodic chamber to prevent scavenging of electrons by oxygen.

From Fig. 6, it is evident that COD removal is proportional to wastewater concentration. The maximum COD removal of 89 % was recorded at the highest COD concentration ( $3400 \text{ mg L}^{-1}$ ). This observation is consistent with the findings by Wang et al. (2008), where COD



**Fig. 5** Effects of wastewater COD concentration on CE and COD removal

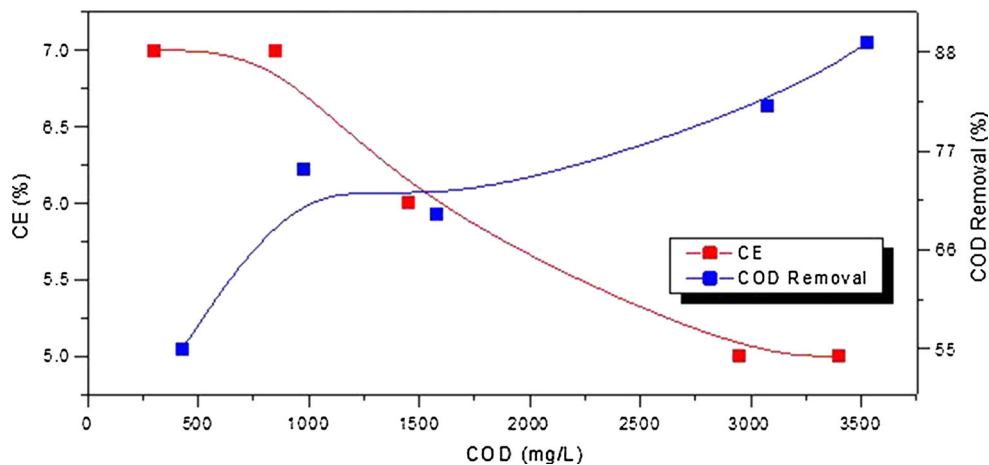
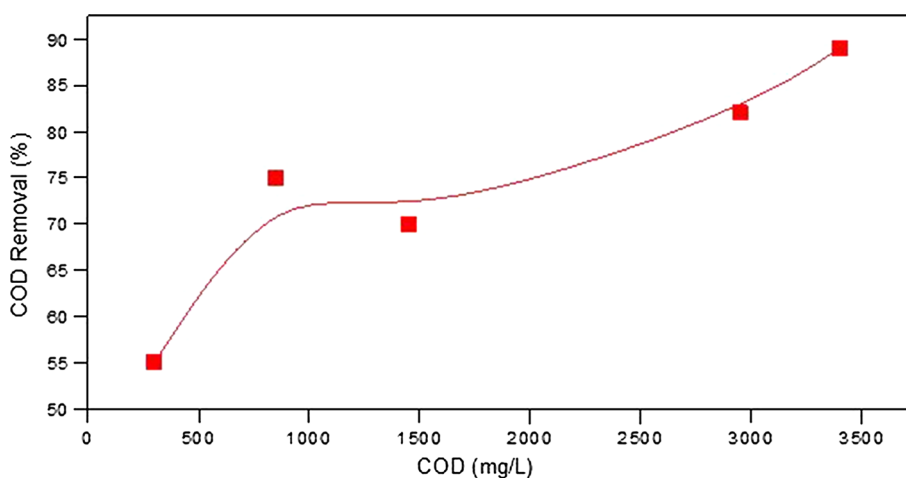


**Fig. 6** Wastewater concentration effect on COD removal



removal increased with wastewater concentration, resulting in a maximum COD removal of 87 % at the highest wastewater COD concentration of 2339 mg L<sup>-1</sup>. Also, considering the volume of wastewater in the anode chamber (1.5 L) and the fact that full-strength wastewater was employed (at the maximum COD concentration reported, 3400 mg L<sup>-1</sup>), this result shows the potential of the MFC as a wastewater treatment technique.

**Characterization result of electrode**

*Electrochemical analysis*

The cathode OCP was 0.343 mV versus Ag/AgCl. This result was higher than the cathode OCP of 0.230 V versus

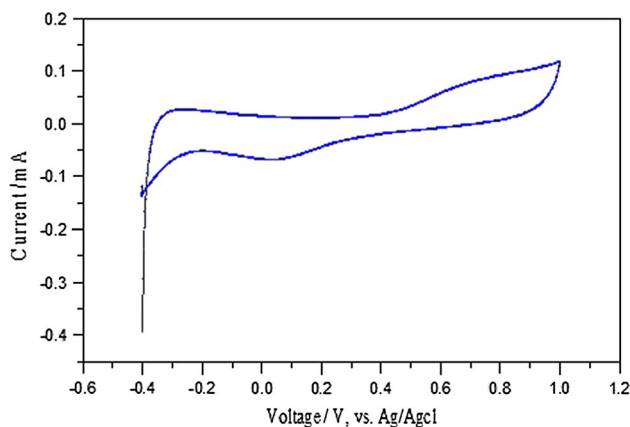


**Fig. 7** CV of SS mesh cathode in cathode solution

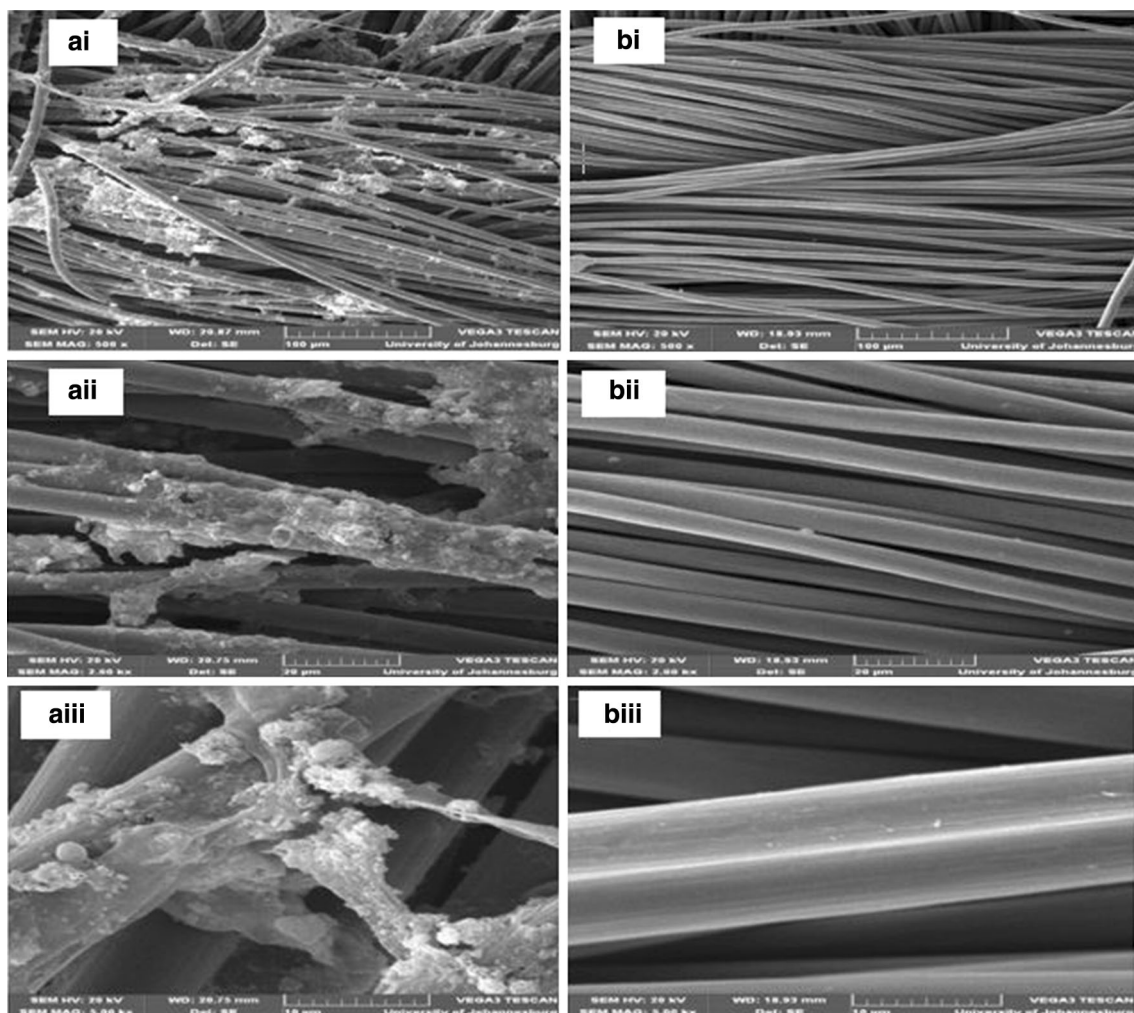


**Fig. 8** Scanning electron micrograph of anode (working electrode) inoculated with domestic wastewater (**a**) and **b** a control electrode (before inoculation)

Ag/AgCl reported by Liu and Logan (2004) when the MFC was operated without a PEM. An average open circuit voltage (OCV) of  $0.735 \pm 0.1$  V was recorded, a result that is fairly close to the maximum OCV of 0.8 V reported in single-chamber MFCs using oxygen as electron acceptor (Cheng and Logan 2007).

The appearance of capacitive currents and faradaic peaks in the CV (Fig. 7) suggests that the electrode (stainless steel mesh cathode) is conducting and is suitable for MFC application.

#### Scanning electron micrograph analysis of anode

The scanning electron micrograph results of the surface morphology of the anode are depicted in Fig. 8. The result

reveals the growth of biofilm on the working electrode (Fig. 8a i–iii) at different magnifications compared with none on the control electrode (Fig. 8b i–iii). This indicates the colonization of the electrode by the bacteria consortia in the wastewater (Park et al. 2005). The exoelectrogenic bacteria in the wastewater are believed to be responsible for the anodic oxidation reaction leading to electricity generation (Muthukumar and Sangeetha 2014).

#### Conclusion

A relatively low-cost sandwich dual-chamber microbial fuel cell (MFC) was constructed for energy generation and domestic wastewater treatment. The successful





incorporation of the sandwich electrode membrane electrode configuration and an uncatalyzed mesh current collector cathode into the dual-chamber MFC increased power production and wastewater treatment efficiency and at the same time reduced the cost. Furthermore, the use of a relatively larger reactor (1.5 L empty bed volume), compared with most of the MFCs reported in the literature, lends credence to the upscaling potential of this reactor for full-scale energy generation and wastewater treatment.

**Acknowledgments** The University of Johannesburg is gratefully acknowledged for supporting this project. This research was co funded with National Research Fund (NRF) THRIP Grant UID: 90260 and ESKOM Grant (Energy generation from Microbial Fuel Cell). Also, the Young Water Professional (YWP), South Africa is acknowledged for facilitating a research writing workshop at the University of Johannesburg in January 2014 where the first author was further exposed to the art of writing scientific articles.

## References

- Bahadoorsingh P (2010) Comparison of nitrification activity in membrane and conventional enhanced biological phosphorus removal processes. PhD Thesis, University of British Columbia
- Cheng S, Logan BE (2007) Ammonia treatment of carbon cloth anodes to enhance power generation of microbial fuel cells. *Electrochem Commun* 9:492–496
- Cheng S, Liu H, Logan BE (2006) Increased power generation in a continuous flow MFC with advective flow through the porous anode and reduced electrode spacing. *Environ Sci Technol* 40:2426–2432
- Fan Y, Hu H, Liu H (2007) Sustainable power generation in microbial fuel cells using bicarbonate buffer and proton transfer mechanisms. *Environ Sci Technol* 41:8154–8158
- Feng Y, Wang X, Logan BE, Lee H (2008) Brewery wastewater treatment using air–cathode microbial fuel cells. *Appl Microbiol Biotechnol* 78:873–880
- He Z, Minter SD, Angenent LT (2005) Electricity generation from artificial wastewater using an up flow microbial fuel cell. *Environ Sci Technol* 39:5262–5267
- Kiely PD, Rader G, Regan JM, Logan BE (2011) Long-term cathode performance and the microbial communities that develop in microbial fuel cells fed different fermentation end products. *Bioresour Technol* 102:361–366
- Liu H, Logan BE (2004) Electricity generation using an air–cathode single chamber microbial fuel cell in the presence and absence of a proton exchange membrane. *Environ Sci Technol* 38:4040–4046
- Liu H, Cheng S, Logan BE (2005) Production of electricity from acetate or butyrate using a single-chamber microbial fuel cell. *Environ Sci Technol* 39:658–662
- Logan BE (2008) *Microbial fuel cells*. Wiley, New Jersey
- Logan BE (2012) Essential data and techniques for conducting microbial fuel cell and other types of bio electrochemical system experiments. *ChemSusChem* 5:988–994
- Logan BE, Hamelers B, Rozendal R, Schrorder U, Keller J, Freguia S, Aelterman P, Verstraete W, Rabaey K (2006) Microbial fuel cells: methodology and technology. *Environ Sci Technol* 40:5181–5192
- Luo Y, Zhang F, Wei B, Liu G, Zhang R, Logan BE (2011) Power generation using carbon mesh cathodes with different diffusion layers in microbial fuel cells. *J Power Sources* 196:9317–9321
- Min B, Logan B (2004) Continuous electricity generation from domestic wastewater and organic substrates in flat plate microbial fuel cell. *Environ Sci Technol* 38:5809–5814
- Min B, Kim JR, Oh SE, Regan JM, Logan BE (2005) Electricity generation from swine wastewater using microbial fuel cell. *Water Res* 39:4961–4968
- Miura Y, Hiraiwa MN, Ito T, Itonaga T, Watanabe Y, Okabe S (2007) Bacterial community structures in MBRs treating municipal wastewater: relationship between community stability and reactor performance. *Water Res* 41:627–637
- Moon H, Chang IS, Kim BH (2006) Continuous electricity production from artificial wastewater using a mediator-less microbial fuel cell. *Bioresour Technol* 97:621–627
- Muthukumar M, Sangeetha T (2014) The harnessing of bioenergy from a dual chambered microbial fuel cell (MFC) employing sago-processing wastewater as catholyte. *Int J Green Energy* 11:161–172
- Park HI, Choi Y, Pak D (2005) Nitrate reduction using an electrode as direct electron donor in a biofilm-electrode reactor. *Process Biochem* 40:3383–3388
- Rodrigo M, Cañizares P, Lobato J, Paz R, Sáez C, Linares J (2007) Production of electricity from the treatment of urban wastewater using a microbial fuel cell. *J Power Sources* 169:198–204
- Wang X, Feng Y, Lee H (2008) Electricity production from beer brewery wastewater using single chamber microbial fuel cell. *Water Sci Technol* 57:1117–1122
- Wang X, Feng Y, Wang H, Qu Y, Yu Y, Ren N, Li N, Wang E, Lee H, Logan BE (2009) Bioaugmentation for electricity generation from corn stover biomass using microbial fuel cells. *Environ Sci Technol* 43:6088–6093
- Wen Q, Wu Y, Cao D, Zhao L, Sun Q (2009) Electricity generation and modelling of microbial fuel cell from continuous beer brewery wastewater. *Bioresour Technol* 100:4171–4175
- Xia X, Zhang F, Zhang X, Liang P, Huang X, Logan BE (2013) Use of pyrolyzed iron ethylenediaminetetraacetic acid modified activated carbon as air–cathode catalyst in microbial fuel cells. *ACS Appl Mater Interfaces* 5:7862–7866
- You S, Zhao Q, Zhang J, Jiang J, Zhao S (2006) A microbial fuel cell using permanganate as the cathodic electron acceptor. *J Power Sources* 162:1409–1415
- Zhang F, Cheng S, Pant D, Van Bogart G, Logan BE (2009) Power generation using an activated carbon and metal cathode in a microbial fuel cell. *Electrochem Commun* 11:2177–2179
- Zhang F, Saito T, Cheng S, Hickner MA, Logan BE (2010) Microbial fuel cell cathodes with poly (dimethyl siloxane) diffusion layers constructed around stainless steel mesh current collectors. *Environ Sci Technol* 44:1490–1495



- Zhang F, Merrill MD, Tokash JC, Saito T, Cheng S, Hickner MA, Logan BE (2011) Mesh optimization for microbial fuel cell cathodes constructed around stainless steel mesh current collectors. *J Power Sources* 196:1097–1102
- Zhong C, Zhang B, Kong L, Xue A, Ni J (2011) Electricity generation from molasses wastewater by an anaerobic baffled stacking microbial fuel cell. *J Chem Technol Biotechnol* 86:406–413

